

**Traffic congestion and the lifetime of networks with moving nodes**Xianxia Yang,<sup>1</sup> Jie Li,<sup>1</sup> Cunlai Pu,<sup>1,2,\*</sup> Meichen Yan,<sup>1</sup> Rajput Ramiz Sharafat,<sup>1</sup> Jian Yang,<sup>1</sup>  
Konstantinos Gakis,<sup>2</sup> and Panos M. Pardalos<sup>2</sup><sup>1</sup>*Department of Computer Science and Engineering, Nanjing University of Science and Technology, Nanjing 210094, China*<sup>2</sup>*Industrial and Systems Engineering, University of Florida, Gainesville, Florida, USA*

(Received 24 April 2016; revised manuscript received 17 October 2016; published 23 January 2017)

For many power-limited networks, such as wireless sensor networks and mobile ad hoc networks, maximizing the network lifetime is the first concern in the related designing and maintaining activities. We study the network lifetime from the perspective of network science. In our model, nodes are initially assigned a fixed amount of energy moving in a square area and consume the energy when delivering packets. We obtain four different traffic regimes: no, slow, fast, and absolute congestion regimes, which are basically dependent on the packet generation rate. We derive the network lifetime by considering the specific regime of the traffic flow. We find that traffic congestion inversely affects network lifetime in the sense that high traffic congestion results in short network lifetime. We also discuss the impacts of factors such as communication radius, node moving speed, routing strategy, etc., on network lifetime and traffic congestion.

DOI: [10.1103/PhysRevE.95.012322](https://doi.org/10.1103/PhysRevE.95.012322)**I. INTRODUCTION**

Nowadays, human life is increasingly dependent on a variety of information infrastructures, such as the Internet, mobile communication networks, sensor networks, ad hoc networks, and others. Meanwhile, these technological networks face challenging problems including traffic congestion [1–3], cascading failures [4–7], errors and attacks [8–11], and virus spreading [12–17], which have been widely discussed in the network science community. In those communication networks, when the nodes' packet generation rate is small, the volume of traffic going into the network and coming out of the network achieve equilibrium. However, when the packet generation rate exceeds a critical value, nodes cannot manage to deliver their buffered packets, and thus the overall network traffic load increases with time, which is recognized as the general congestion state of traffic flows. The critical packet generation rate corresponding to the onset of traffic congestion is often used as an indicator of the maximum capacity of the network [18–21].

Essentially, the network capacity is mostly determined by the network topological structures. It was found that scale-free networks are more susceptible to traffic congestion than homogenous networks [22,23]. The heterogeneous degree distribution of scale-free networks is prone to cause uneven traffic load distribution, in which large-degree nodes usually process a larger amount of traffic load than small-degree nodes. Thus, the congestion phenomenon usually starts at large degree nodes and then spreads to the whole network. Since many real-world complex networks especially communication networks are scale-free networks [24], researchers proposed various improved strategies [18], which can be classified into “hard” and “soft” strategies in order to alleviate traffic congestion and enhance the capacity of scale-free networks. The hard strategies are about optimizing network topological structures by removing some links or nodes such as the high-degree-first (HDF) strategy [25], the high-betweenness-first (HBF)

strategy [26], and the variance-of-neighbor-degree-reduction (VNDR) strategy [27], or by adding some links between nodes with long distance or nodes in the same neighborhood of large-degree nodes [28]. The limitation of the hard strategies is that in real situation it is often costly or even impossible to modify the network topological structures. The soft strategies are various routing protocols more applicable to real-world communication networks. The well-known shortest path protocol [29] transmits packets along the shortest paths to destination nodes. However, the shortest paths usually intersect on a few large-degree nodes, which are vulnerable to traffic congestion. The other improved routing protocols consider not only path length when choosing the optimal delivery paths, but also node degree [22,30,31], node load [32–36], memory information [37], next-nearest neighbors [38,39], and the like. Generally, the more information considered in path selection, the better performance the protocol has and the larger the computational cost is. In addition, some of those improved protocols use tunable control parameters in their cost functions to explore the maximum transmission performance. Recently, researchers began to study transport processes on multilayer [40–43] or multiplex networks [44–46] with emphasis on optimizing the network capacity and transmission efficiency.

Besides the fixed communication infrastructures well discussed in the field of network science, there is another broad type of communication networks, which are usually deployed in adverse environments to perform special tasks [47–52]. The nodes in such kinds of networks can be mobile or have a certain level of mobility and are dynamically self-organized without fixed infrastructure. In addition, the nodes are often powered by small battery and die when they run out of power [53]. The most straightforward examples are sensor nodes in wireless sensor networks and robots in the multirobot networks. Recently, Yang *et al.* [54] proposed an adaptive routing strategy to improve traffic capacity of dynamical networks, in which the nodes are moving, and the links can exist only when the distances of nodes meet the communication constraints. However, for those power-limited networks, the biggest concern is how to make good use of the energy and prolong the network lifetime, which needs to

\*pucunlai@njust.edu.cn

be further explored from the perspective of network science. In this paper, we study traffic congestion and the lifetime of networks consisting of power-limited mobile nodes. We further look into the traffic congestion phenomenon and obtain four different congestion states. Then we derive the network lifetime based on the state of traffic congestion. We also study how factors such as packet generation rate, communication radius, and node speed affect the network lifetime and traffic congestion.

## II. THE NETWORK MODEL

We generate the dynamical networks following Ref. [54]. We first set a  $L \times L$  square area with periodic boundary conditions in the Euclidean space. At time  $t = 0$ , we randomly add  $N$  moving nodes into the square area. Assuming that  $x_i(t)$  [ $y_i(t)$ ] is the  $x$  coordinate ( $y$  coordinate) of node  $i$  at time  $t$ , and  $\theta_i(t)$  denotes the moving direction of node  $i$  at time  $t$ .  $x_i(0)$  [ $y_i(0)$ ] is randomly selected from the interval  $[0, L]$ .  $\theta_i(0)$  is randomly selected from the interval  $[-\pi, \pi]$ . Since the nodes are moving, their positions change with time  $t$ . For instance, the evolution of node  $i$ 's coordinates are the following:

$$\begin{aligned} x_i(t+1) &= x_i(t) + v \cos \theta_i(t), \\ y_i(t+1) &= y_i(t) + v \sin \theta_i(t), \\ \theta_i(t+1) &= \theta_i(t) + \phi_i(t). \end{aligned} \quad (1)$$

Where  $v$  (a constant value) represents the moving speed, which is identical for all the nodes.  $\phi_i(t)$  represents the change of moving direction of node  $i$  between time  $t+1$  and time  $t$ , which is randomly selected from the interval  $[-\pi, \pi]$ . Then the Euclidean distance between two nodes  $i$  and  $j$  at time  $t$  is calculated as follows:

$$l_{ij}(t) = \sqrt{[x_i(t) - x_j(t)]^2 + [y_i(t) - y_j(t)]^2}. \quad (2)$$

All nodes have the same communication radius  $r$ , and any two nodes are connected by a temporal link (communication channel) when their instantaneous distance is no greater than  $r$ . Then the temporal neighbor set of node  $i$  contains all the nodes in node  $i$ 's current communication area.

## III. THE TRAFFIC MODEL

In our traffic model, the role of all nodes is identical, which can create, buffer, deliver, and receive packets. Specifically, every node generates packets with rate  $\rho$ , thus at each time step there are on average  $N\rho$  packets inserted into the network. The packets' destination nodes are randomly selected from the network. Every node has an infinite queue with the first-in-first-out (FIFO) rule for buffering packets. Each node has  $E_0$  units of energy at the beginning. A node can deliver at most  $C$  packets at each time step. The one-hop delivery of a packet costs  $\Delta E$  units of energy. If the destination node is a neighbor of the node the packet currently visits, at the next time step the packet will be directly delivered to the destination node and then be removed immediately. Otherwise the current node needs to deliver the packet to the appropriate neighbor node chosen based on a given routing strategy. Assuming that at time  $t$  the packet is in node  $s$ , and the destination node  $d$  is not a neighbor of  $s$ , then node  $s$  will send the packet to its

neighbor node  $i$  with the following probability:

$$P_{si}(t) = \left[ \frac{E_i(t)}{\sum_j E_j(t)} \right]^{1-\alpha} \bigg/ \left[ \frac{l_{id}(t)}{\sum_j l_{jd}(t)} \right]^\alpha, \quad \alpha \in [0, 1], \quad (3)$$

where  $E_i(t)$  is the residual energy of  $i$  at time  $t$ . The sums in the equation run over the temporal neighbors of node  $s$ , and  $\alpha$  is a tunable parameter ranging from 0 to 1. When  $\alpha = 0$ , the probability of selecting neighbor node  $i$  is proportional to  $i$ 's residual energy. When  $\alpha = 1$ , the probability of selecting neighbor node  $i$  is inversely proportional to the distance between node  $i$  and node  $d$ . When  $0 < \alpha < 1$ , the node distance and residual energy together determine the next hop node. If there are currently no neighbor nodes, node  $s$  will keep the packet and deliver it later. As time goes by, the residual energy of nodes decreases. The definition of network lifetime is flexible and usually application specific. For simplification purposes, we assume that the lifetime of the network is from the beginning until the first-dying node appears, which follows Ref. [55] closely.

## IV. NETWORK CONGESTION

Ideally, when the delivery capacity of nodes is infinite, there is no traffic congestion phenomenon. However, the delivery capacity is always limited in real situations, and the traffic congestion arises when the network is unable to deal with the continuously injected traffic. Previously, traffic flow was considered with only two states [18–20]. When the packet generation rate  $\rho$  is not greater than the critical value, the number of packets  $S(t)$  in the network is generally constant after a very short transition time, and the traffic is under a free flow state. When  $\rho$  is larger than the critical value,  $S(t)$  increases with time, which is taken as the traffic congestion state. However, when we consider more real-world constraints in the traffic model, we may obtain more traffic states. For instance, if we assume that the node queue has finite size with a last-in-first-out rule, three traffic states, free-flow, jamming, and congested traffic regimes, are obtained [56].

In our work, we consider the energy-limited dynamical network, and obtain four different traffic states, of which the definition is as follows:

(1) No congestion state: The number of packets is constant during the lifetime of the network. There is no congested node during the lifetime of the network. Note that there might be temporal congested node, and the number of packets may show some fluctuation. When  $\rho$  is very small, the network is under no congestion state.

(2) Slow congestion state: The number of packets increases nonlinearly during the lifetime of the network. The number of congested nodes gradually increases until the network dies, but some nodes are not congested at the end. When  $\rho$  is larger than the critical value  $\rho_s$  of slow congestion state, the network will undergo the slow congestion state.

(3) Fast congestion state: The number of packets increases nonlinearly first and then linearly until the network dies. The number of congested nodes increases with time, and all nodes become congested at the end of the network. When  $\rho$  is larger than the critical value  $\rho_f$  of fast congestion state, the network will undergo the fast congestion state.

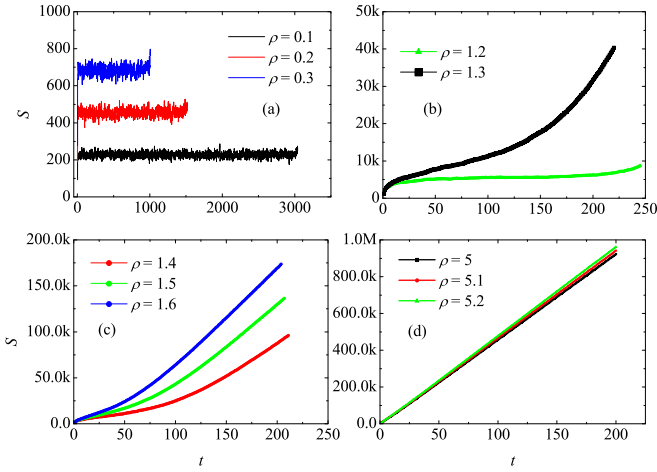


FIG. 1.  $S$  vs  $t$  in different traffic states: (a) no congestion state, (b) slow congestion state, (c) fast congestion state, and (d) absolute congestion state. The simulation parameters are  $N = 1000$ ,  $L = 20$ ,  $r = 3$ ,  $v = 0.5$ ,  $\alpha = 0.5$ ,  $\tau_0 = 3.275$ ,  $C = 5$ ,  $E_0 = 1000$ , and  $\Delta E = 1$ . The curves are placed so that the curve of a smaller  $\rho$  is in a lower position.

(4) Absolute congestion state: The number of packets increases linearly from the beginning until the end. After the first few steps, all nodes are congested until the network dies. When  $\rho$  is larger than the critical value  $\rho_a$  of the absolute congestion state, the network will undergo the absolute congestion state.

We show the different congestion states with simulation results in Figs. 1 and 2. In Fig. 1(a), when  $\rho$  is very small,  $S(t)$  increases abruptly at the first few time steps and then generally keeps constant until the network dies, which is the no congestion state. According to Fig. 2(a), in the no congestion state, the number of congested nodes  $n_c$  is 0, but the temporal congestion of nodes is allowed, which is why there are small fluctuations in the results of  $n_c$  and  $S(t)$ . As  $\rho$  increases and surpasses the first critical value  $\rho_s$ ,  $S(t)$  increases nonlinearly

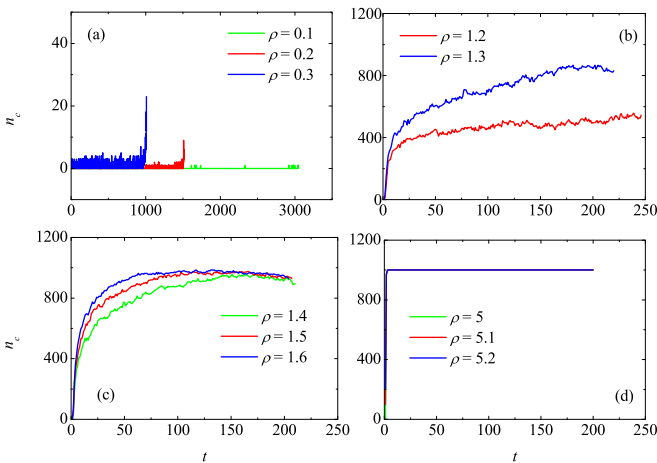


FIG. 2.  $n_c$  vs  $t$  in different traffic states: (a) no congestion state, (b) slow congestion state, (c) fast congestion state, and (d) absolute congestion state. The simulation parameters are as in Fig. 1. The curves are placed so that the curve of a smaller  $\rho$  is in a lower position.

TABLE I. Possible time periods in the whole network lifetime.

Time period	Number of congested nodes $n_c$	Number of packets $S$
$T_1$	$n_c = 0$	Constant
$T_2$	$0 < n_c < N$	Nonlinear increase
$T_3$	$n_c = N$	Linear increase

until the network dies, which is the slow congestion state, shown in Fig. 1(b). We see from Fig. 2(b) that in the slow congestion state, a fraction of nodes becomes congested first, and then more and more nodes become congested, but when the network dies there are still noncongested nodes. Note that there are “tilting tails” in the curves for the no and slow congestion states as demonstrated in Figs. 1(a), 1(b), 2(a), and 2(b). The cause of the tilt-tail effect is that, in the last several steps, the residual energy of most nodes is very low, and according to our routing strategy, the packets will be delivered to a few nodes of relatively high residual energy, which makes the traffic load of those nodes substantially increase. When  $\rho$  further increases and surpasses the second critical value  $\rho_f$ ,  $S(t)$  increases nonlinearly and then linearly with time, which is the fast congestion state, as shown in Fig. 1(c). We see from Fig. 2(c) that in the fast congestion state, first a fraction of nodes becomes congested, and then the congestion gradually spreads to all nodes. When  $\rho$  is larger than the third critical value  $\rho_a$ ,  $S(t)$  almost increases linearly from the beginning, which is the “absolute congestion” state, as shown in Fig. 1(d). We see from Fig. 2(d) that in the absolute congestion state, almost all nodes are congested at the beginning. Note that for the fast and absolute congestion states, there are no tilt-tail effects, because near the end of the life of the network, all nodes are congested and the residual energy of nodes has no significant difference.

To further illustrate the different congestion states, we divide the whole network lifetime  $T$  into three periods of time,  $T_1$ ,  $T_2$ , and  $T_3$ , which are shown in Table I. We have  $T = T_1 + T_2 + T_3$ . Then the different congestion states for the whole network lifetime are shown in Table II.

In addition, we provide the analytical results of  $S(t)$  and  $n_c(t)$  in the Appendix, based on which we can also obtain the different traffic states.

## V. NETWORK LIFETIME

According to Eq. (3), nodes deliver the packets to the neighbor nodes of high residual energy with large probability. In this case, high residual energy nodes consume their energy faster than low residual energy nodes, which leads to a relatively even distribution of the residual energy. We define the range of energy at time  $t$  as

$$R(t) = E_{\max}(t) - E_{\min}(t), \quad (4)$$

where  $E_{\max}(t)$  ( $E_{\min}(t)$ ) is the maximum (minimum) node residual energy at time  $t$ . At the time  $T$  when the network dies, we have  $E_{\min}(T) = 0$  and  $R(T) = E_{\max}(T)$ . Then, the network lifetime  $T$  is calculated as follows:

$$T = \frac{E_{\text{total}}(0) - E_{\text{total}}(T)}{D * \Delta E}, \quad (5)$$

TABLE II. Types of congestion state.

Congestion state	$T_1$	$T_2$	$T_3$	$T$	$n_c$	$S$	Critical value of $\rho$
No	$\neq 0$	0	0	$T = T_1$	$n_c = 0$	Constant	0
Slow	0	$\neq 0$	0	$T = T_2$	$0 < n_c < N$	Nonlinear increase	$\rho_s$
Fast	0	$\neq 0$	$\neq 0$	$T = T_2 + T_3$	$0 < n_c \leq N$	Nonlinear+linear increase	$\rho_f$
Absolute	0	0	$\neq 0$	$T = T_3$	$n_c = N$	Linear increase	$\rho_a$

where  $E_{\text{total}}(t)$  is the total units of energy at time  $t$ .  $E_{\text{total}}(0) = NE_0$ . Since the residual energy is approximately evenly distributed among nodes,  $E_{\text{total}}(T) \approx N \times [E_{\text{max}}(T) + E_{\text{min}}(T)]/2 = NR(T)/2$ .  $D$  is the average number of packets sent by all the nodes in a time step.

In the no congestion state,  $D = N\rho\tau_0$ , where  $\tau_0$  is the characteristic transmission time, which equals the average number of transmission hops from source node to destination node. Note that  $\tau_0$  is generally not equal to the average transmission time, which usually contains the time waiting for delivery. Then the network lifetime  $T$  for the no congestion state is calculated as follows:

$$T = \frac{E_{\text{total}}(0) - E_{\text{total}}(T)}{D * \Delta E} = \frac{NE_0 - NR(T)/2}{N\rho\tau_0 * \Delta E} = \frac{E_0 - R(T)/2}{\rho\tau_0\Delta E}. \quad (6)$$

In the absolute congestion state, we have  $S(t) > D = N * C$ . Almost all nodes are congested from the beginning, and every node delivers  $C$  packets at each time step. Therefore, all nodes consume the energy with the same rate. When the network dies, the total residual energy of nodes is close to zero:  $E_{\text{total}}(T) \approx 0$  or  $R(T) \approx 0$ . Note that when  $\rho > C$ , all nodes are congested at the very beginning, and in this case,  $E_{\text{total}}(T)$  and  $R(T)$  are definitely 0. Then the network lifetime  $T$  for the absolute congestion state is

$$T = \frac{E_{\text{total}}(0) - E_{\text{total}}(T)}{D * \Delta E} \approx \frac{NE_0}{NC\Delta E} \approx \frac{E_0}{C\Delta E}. \quad (7)$$

For the slow and fast congestion states, there are time periods of nonlinear increase of  $S(t)$ , when  $D(N\rho\tau_0 < D < NC)$  increases with time, but this is hard to estimate precisely. In addition, it is not possible to calculate the duration time of the tilt-tail effects in the slow congestion state. For all these reasons, we set a nonlinear parameter  $k$  to measure the compositive effects of those unpredictable factors on network lifetime  $T$ . The general formula of  $T$  for all the traffic states is given as follows:

$$T = k \frac{E_0}{\Omega * \Delta E}, \quad \Omega = \min\{\rho\tau_0, C\}. \quad (8)$$

For the no congestion state,  $D = N\rho\tau_0 < NC$ ,  $\rho\tau_0 < C$ , we have  $k = \frac{E_0 - R(T)/2}{E_0} \rightarrow 1$ . For the absolute congestion state,  $D = NC < N\rho\tau_0$ ,  $C < \rho\tau_0$ , we have  $k = 1$ . For the slow and fast congestion states,  $k$  depends on the nonlinear factors. For the slow congestion state,  $\rho\tau_0 < C$ , then  $\Omega = \rho\tau_0$ . For the

fast congestion state,  $\Omega$  is dependent on  $\rho$ . When  $\rho < C/\tau_0$ ,  $\Omega = \rho\tau_0$ , otherwise,  $\Omega = C$ .

## VI. SIMULATION RESULTS

We study the impacts of factors on traffic congestion and network lifetime through simulation. The key factors of our model include packet generation rate  $\rho$ , communication radius  $r$ , node speed  $v$ , routing parameter  $\alpha$ , area size  $L$ , and network size  $N$ .  $\phi_i(t)$  is bounded in range  $[-\pi/3, \pi/3]$  in the simulation for simplification purpose. Previously, we usually have used the typical order parameter [21] to quantify the phase transition

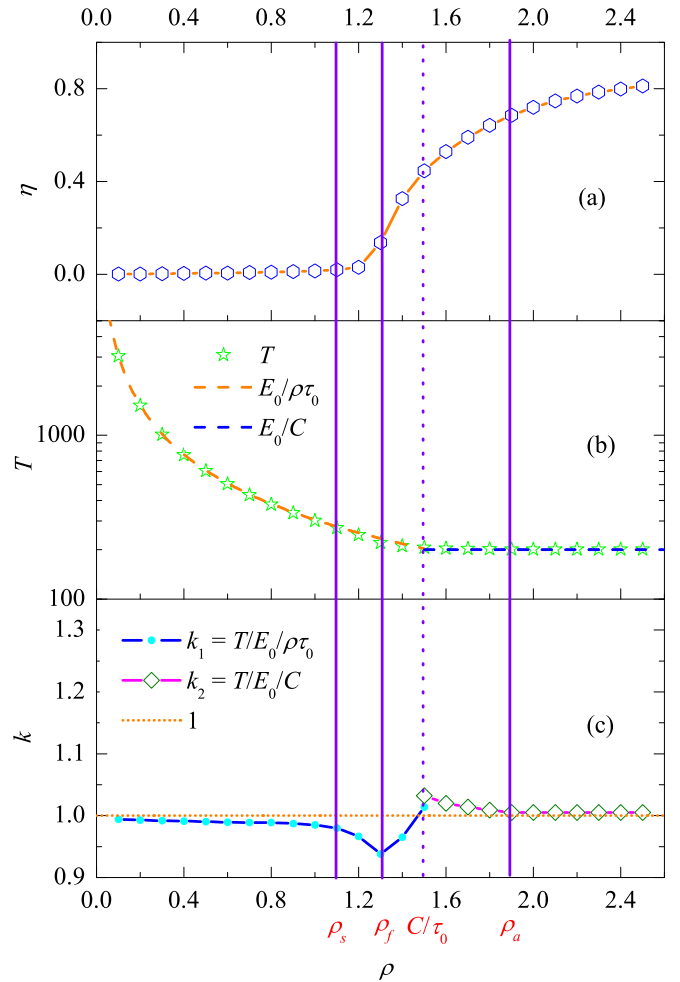


FIG. 3. (a)  $\eta$ , (b)  $T$ , and (c)  $k$  vs  $\rho$ .  $\rho_s$ ,  $\rho_f$ , and  $\rho_a$  are the critical values for slow, fast, and absolute congestion states, respectively. The simulation parameters are as in Fig. 1. The results are the average of 1000 independent runs.



of traffic load in the network. Here we slightly modify the typical order parameter to apply it to our model, which is given as follows:

$$\eta = \frac{1}{\rho N \Delta t} \sum_{t=0}^{T-\Delta t} \frac{S(t + \Delta t) - S(t)}{T - \Delta t + 1}, \quad (9)$$

where the meaning of  $\rho$ ,  $S(t)$ ,  $N$ , and  $T$  is the same as above.  $\Delta t$  is the elementary time slot for comparing traffic load,  $1 \leq \Delta t \leq T$ . Note that in our model, the network lifetime  $T$  is always a finite value, and in the simulation, we set  $\Delta t = 1$ .  $\eta$  is in fact the ratio of the average increment of traffic load during time  $\Delta t$  to the amount of traffic inserted into the network during time  $\Delta t$ . We know that  $0 \leq \eta \leq 1$ . When  $\rho$  is no greater than  $\rho_s$ , there is no traffic congestion, and we have  $\eta = 0$ , while when  $\rho$  is larger than  $\rho_s$ ,  $\eta > 0$ , and there is traffic congestion.

According to the above analytic results, packet generation rate  $\rho$  has significant influence on the traffic congestion and network lifetime. We first study the impact of  $\rho$  by fixing the other parameters as follows: network size  $N = 1000$ , routing parameter  $\alpha = 0.5$ , node speed  $v = 0.5$ , communication radius  $r = 3$ , area size  $L = 20$ , node delivery capacity  $C = 5$ , and node's initial units of energy  $E_0 = 1000$ , per node energy consumption rate  $\Delta E = 1$ . Based on these parameters, we obtain the characteristic transmission time  $\tau_0 = 3.275$  through simulation.

In Fig. 3(a) we see that in the no congestion state ( $\rho \leq \rho_s$ ),  $\eta = 0$ , when  $\rho$  surpasses  $\rho_s$ ,  $\eta$  increases and then converges with  $\rho$ . In Fig. 3(b), with the increase of  $\rho$ ,  $T$  first decreases greatly, and then gradually converges to the minimum value  $T = 200$ . The reason for the results in Fig. 3(b) is that, when we increase the packet generation rate, more packets are injected into the network at each time step, and thus more energy is

consumed in each time step, so therefore the network lifetime decreases accordingly. When the network is under the absolute congestion state ( $\rho > \rho_a$ ), the energy consumed in each time step is nearly constant, and thus the network lifetime is a constant value, which can also be inferred from Eq. (7). Moreover, in Fig. 3(b) the analytical and simulation results agree very well with each other. In Fig. 3(c), we see that when the network is in the no congestion state, the nonlinear parameter  $k$  is smaller than but very close to 1. When the network is in the absolute congestion state,  $k$  is equal to 1. When the network is in the slow or fast congestion state,  $k$  deviates from 1, which are consistent with the above analytical analysis.

The other factors, such as the communication radius  $r$ , node speed  $v$ , and routing parameter  $\alpha$ , do not appear in the above derivation of network lifetime [Eq. (8)]. However, they affect the characteristic transmission time and the range of energy, and thus indirectly affect the network lifetime. Note that when the traffic is under the absolute congestion state, the network lifetime is almost constant and independent of these factors, which can be inferred from Eq. (7). Therefore, we mainly study the impact of these factors when there is almost no traffic congestion in the network. Figures 4(a), 4(b), and 4(c) show the impact of  $r$ . In Fig. 4(b),  $\eta$  is very small, which means that there is almost no traffic congestion in the network. In Fig. 4(a),  $\tau_0$  decreases with  $r$  quickly and then tends to 1. When the communication radius increases, nodes have more neighbor nodes, which makes the transmission hops decrease, and when the communication radius is large enough, each node is directly connected to all the other nodes, and then just one hop is needed to deliver a packet. In Fig. 4(c),  $T$  increases with  $r$  first and then converges. Since the transmission hops decrease with  $r$ , the average energy for delivering a packet decreases, which leads

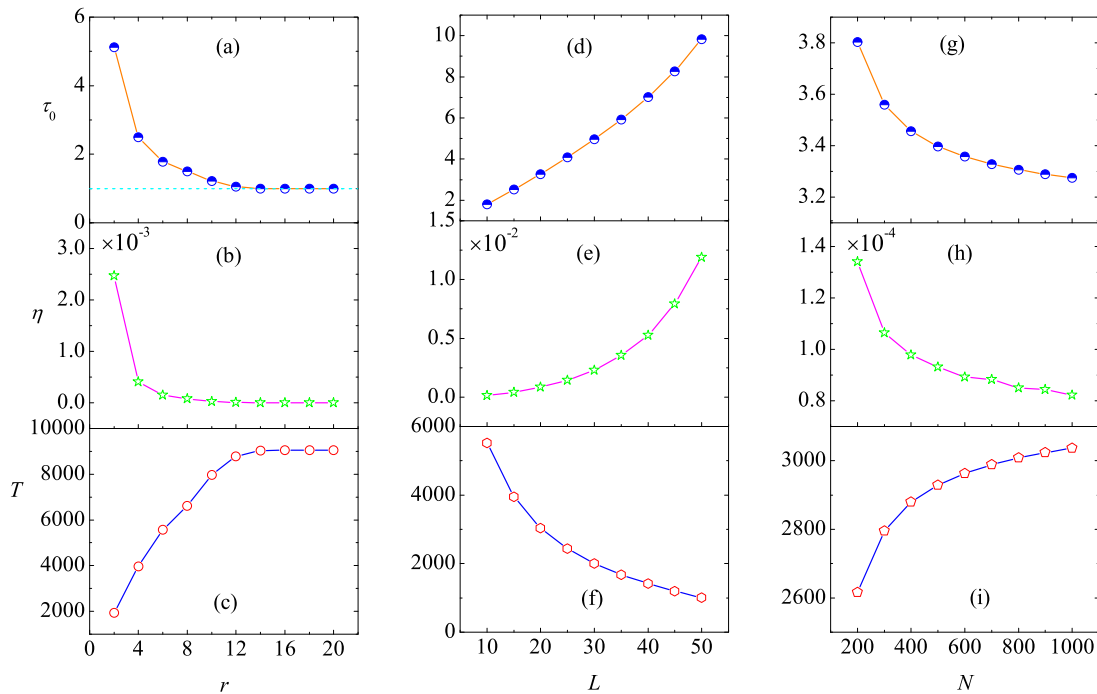


FIG. 4. (a)  $\tau_0$ , (b)  $\eta$ , and (c)  $T$  vs  $r$ ,  $N = 1000, L = 20$ . (d)  $\tau_0$ , (e)  $\eta$ , and (f)  $T$  vs  $L$ ,  $N = 1000, r = 3$ . (g)  $\tau_0$ , (h)  $\eta$ , and (i)  $T$  vs  $N$ ,  $L = 20, r = 3$ . The other parameters are as follows:  $v = 0.5, \alpha = 0.5, \rho = 0.1, C = 5, E_0 = 1000$ , and  $\Delta E = 1$  for all the subfigures. The results are the average of 1000 independent runs.

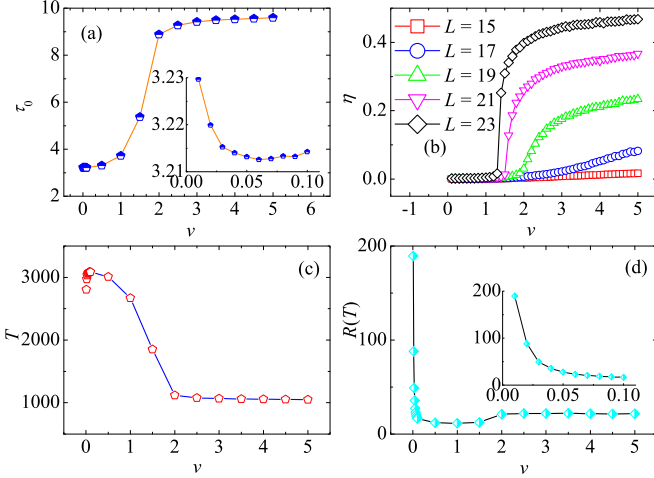


FIG. 5. (a)  $\tau_0$ , (b)  $\eta$ , (c)  $T$ , and (d)  $R(T)$  vs  $v$ .  $N = 1000$ ,  $L = 20$  for (a), (c), and (d),  $r = 3$ ,  $\alpha = 0.5$ ,  $\rho = 0.1$ ,  $C = 1$ ,  $E_0 = 1000$ , and  $\Delta E = 1$ . The results are the average of 1000 independent runs. The inserts show the results of  $v$  ranging from 0.01 to 0.1.

to the increase of network lifetime. Figures 4(d), 4(e), and 4(f) show the results of  $L$ . Both  $\eta$  and  $\tau_0$  increase with  $L$ , and thus  $T$  decreases with  $L$  accordingly. The effect of increasing  $L$  is equivalent to decreasing  $r$ . Figures 4(g), 4(h), and 4(i) show the impact of  $N$ . With the increase of  $N$ ,  $\eta$  and  $\tau_0$  decrease, and thus  $T$  increases. When there are more nodes in the fixed square area, the network will become more dense, which causes the decrease of the characteristic transmission time.

In Fig. 5(a), when  $v$  increases from very small value,  $\tau_0$  decreases slightly (amplified in the insert) and then increases significantly and converges. In Fig. 5(b), when  $v$  is small,  $\eta = 0$ , but when  $v$  is larger than the critical value,  $\eta$  increases abruptly. There is an obvious phase transition of  $\eta$ . In addition, we can see from Fig. 5(b) that the larger  $L$ , the smaller the critical value of  $v$  and the larger  $\eta$ , which means that a larger square area is more susceptible to traffic congestion. In Fig. 5(c),  $T$  first slightly increases with  $v$ , then decreases

quickly and converges. In Fig. 5(d),  $R(T)$  decreases with  $v$  abruptly, then converges. The decrease of  $\tau_0$  and  $R(T)$  leads to the increase of  $T$ . However, when  $v$  increases further, traffic congestion becomes more and more serious, resulting in the increase of  $\tau_0$  and  $\eta$ , and this further leads to the decrease of  $T$ .

In Fig. 6 when  $\alpha$  increases from zero to nonzero,  $\tau_0$  and  $\eta$  decrease abruptly, leading to a substantial increase of  $T$ .  $R(T)$  first decreases quickly with  $\alpha$  and then increases, which causes  $T$  first to increase and then to decrease with  $\alpha$ .

## VII. CONCLUSION

For a wide range of power-limited communication networks, the biggest concern is network lifetime, which has not received enough attention in network science. In this paper, we discuss both network lifetime and traffic congestion based on the methodology of complex network theory. In our model, all nodes move in a spatial area and have limited communication radius, energy, and delivery capacity, but an infinite queue for simplification purposes. Previously, we considered only the presence of traffic congestion in a network. In this paper, we further study the level of traffic congestion, which is divided into no, slow, fast, and absolute congestion states. Moreover, we derive the network lifetime by considering the level of traffic congestion. Generally, network lifetime is opposite to traffic congestion in that a high level of network congestion corresponds to a small network lifetime. Through analytical and simulation results, we find that when the traffic congestion is slight, network lifetime is mainly determined by packet generation rate, characteristic transmission time, and range of energy. When the traffic congestion level is high, network lifetime is constant and determined by the node delivery capacity. Also, an increase of communication radius causes a decrease of the possibility of traffic congestion and thus increases the network lifetime. The influence of the routing parameter and node speed is not monotonic in that there are optimal routing parameter and optimal node speed leading to the maximum network lifetime. It is worth mentioning that future research may consider other definitions of network lifetime such as the time till a fraction of nodes die or the network partitions.

## ACKNOWLEDGMENTS

This work was supported by the National Natural Science Foundation of China (Grants Nos. 61201173 and 61304154), the Specialized Research Fund for the Doctoral Program of Higher Education of China (Grant No. 20133219120032), the Postdoctoral Science Foundation of China (Grant No. 2013M541673), and the China Postdoctoral Science Special Foundation (Grant No. 2015T80556). P.M.P. was partially supported by the Paul and Heidi Brown Preeminent Professorship in ISE at the University of Florida.

## APPENDIX: ANALYTICAL RESULTS OF THE NUMBER OF PACKETS AND THE NUMBER OF CONGESTED NODES

In the main text, we provide the simulation results of the number of packets and the number of congested nodes to illustrate the different traffic states. Here we take a further

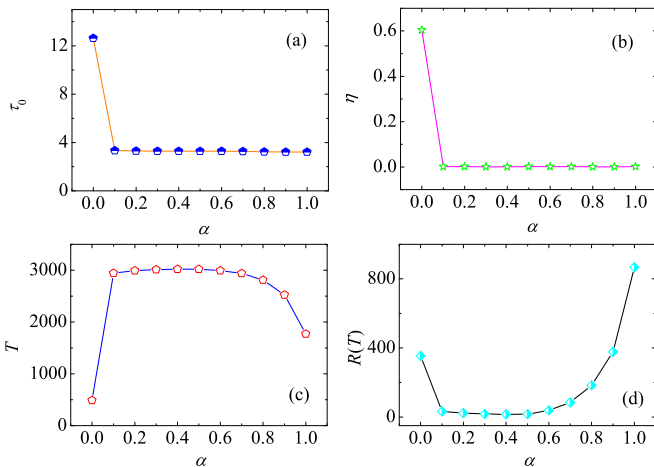


FIG. 6. (a)  $\tau_0$ , (b)  $\eta$ , (c)  $T$ , and (d)  $R(T)$  vs  $\alpha$ .  $N = 1000$ ,  $L = 20$ ,  $r = 3$ ,  $v = 0.01$ ,  $\rho = 0.1$ ,  $C = 5$ ,  $E_0 = 1000$ , and  $\Delta E = 1$ . The results are the average of 1000 independent runs.

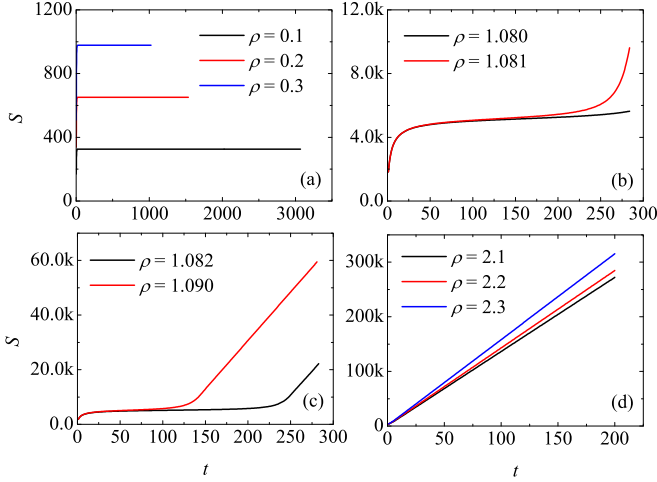


FIG. 7. Number of packets  $S$  vs time step  $t$  for various  $\rho$  for (a) no congestion state, (b) slow congestion state, (c) fast congestion state, and (d) absolute congestion state. The results are obtained through analytical calculation. The parameters are  $N = 1000$ ,  $L = 20$ ,  $r = 3$ ,  $v = 0.5$ ,  $\alpha = 0.5$ ,  $\tau_0 = 3.275$ ,  $C = 5$ ,  $E_0 = 1000$ , and  $\Delta E = 1$ . The curves are placed so that the curve of a smaller  $\rho$  is in a lower position.

step to derive the number of packets  $S$  and the number of congested nodes  $n_c$  as a function of time  $t$ . We assume that, at each time step, each node generates  $N\rho$  packets, deliver  $X$  packets, and a total of  $\beta X$  packets arrive at their destinations, where  $0 \leq \beta \leq 1$ . Furthermore,  $\beta$  is a function of  $t$ . During the stage  $T_1$ ,  $n_c = 0$ , and  $\beta(t)$  is constant and equals  $1/\tau_0$ . During the stage  $T_2$ ,  $n_c$  increases, and  $\beta$  changes with  $t$ . During the stage  $T_3$ ,  $n_c = N$ , and  $\beta$  is constant with  $t$ . Then we assume that the average number of packets in each node queue is  $\lambda(t)$ , and we have  $S(t) = N\lambda(t)$ . For  $\rho > C$ , we have

$$\begin{aligned} S(0) &= N\rho, & \lambda(0) &= \rho, \\ n_c(t) &= N, & X(t) &= NC, \\ \frac{dS}{dt} &= N\frac{d\lambda}{dt} = N\rho - \beta X. \end{aligned} \quad (\text{A1})$$

Through integration, we get  $S(t) = N\lambda(t) = N\rho + (N\rho - \beta X)t = N\rho + N(\rho - \beta C)t$ .

For  $\rho \leq C$ , we have

$$\begin{aligned} S(0) &= N\rho, & \lambda(0) &= \rho, \\ n_c(0) &= 0, & X(0) &= N\rho, \\ \beta(0) &= \frac{1}{\tau_0}. \end{aligned} \quad (\text{A2})$$

Then we get  $S(1) = N(2\rho - \frac{\rho}{\tau_0})$  and  $\lambda(1) = 2\rho - \frac{\rho}{\tau_0}$ . For simplification purposes, we assume that each node queue has  $n$  units of buffers,  $n \rightarrow \infty$ , and each buffer has a packet with the probability  $p$ ,  $p \rightarrow 0$ . Then  $\lambda = np$ . The distribution of number of packets in each queue follows the Poisson distribution,  $P(l) = e^{-\lambda} \frac{\lambda^l}{l!}$ . Then we have  $n_c(t) = N \sum_{l=C+1}^{\infty} P(l) =$

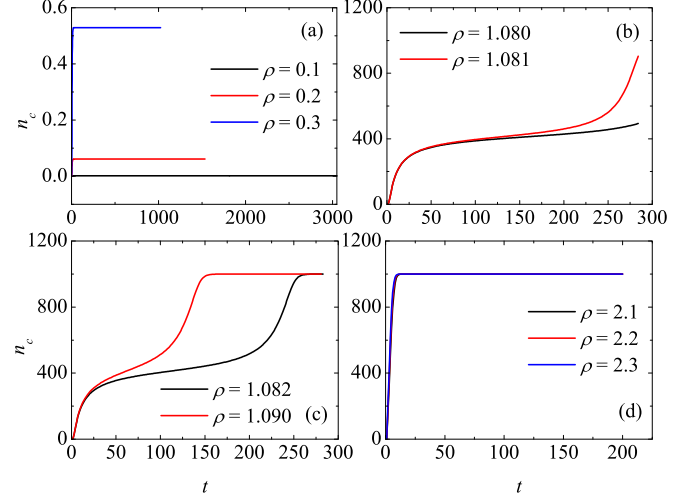


FIG. 8. Number of congested nodes  $n_c$  vs. time step  $t$  for various  $\rho$  for (a) no congestion state, (b) slow congestion state, (c) fast congestion state, and (d) absolute congestion state. The results are obtained through analytical calculation. The parameters are  $N = 1000$ ,  $L = 20$ ,  $r = 3$ ,  $v = 0.5$ ,  $\alpha = 0.5$ ,  $\tau_0 = 3.275$ ,  $C = 5$ ,  $E_0 = 1000$ , and  $\Delta E = 1$ . The curves are placed so that the curve of a smaller  $\rho$  is in a lower position.

$N(1 - \sum_{l=0}^C e^{-\lambda} \frac{\lambda^l}{l!})$ . Furthermore, we obtain that

$$\begin{aligned} X(t) &= n_c(t)C + \sum_{l=0}^C NP(l)l \\ &= n_c(t)C + \sum_{l=1}^C Ne^{-\lambda} \frac{\lambda^l}{l!} \\ &= n_c(t)C + \lambda[N - n_c(t)] - Ne^{-\lambda} \frac{\lambda^{C+1}}{C!}. \end{aligned} \quad (\text{A3})$$

Then for  $t \geq 1$ , we have

$$\begin{aligned} S(1) &= N\left(2\rho - \frac{\rho}{\tau_0}\right), & \lambda(1) &= 2\rho - \frac{\rho}{\tau_0}, \\ n_c(t) &= N\left(1 - \sum_{l=0}^C e^{-\lambda} \frac{\lambda^l}{l!}\right), \\ X(t) &= n_c(t)C + \lambda[N - n_c(t)] - Ne^{-\lambda} \frac{\lambda^{C+1}}{C!}, \\ \frac{dS}{dt} &= N\frac{d\lambda}{dt} = N\rho - \beta X. \end{aligned} \quad (\text{A4})$$

We assume that  $\beta = \frac{1}{\tau_0(\sum_{l=0}^C P(l) + \sum_{l=C+1}^{\infty} P(l)\frac{l}{C})}$ , and based on Eqs. (A1) and (A4), we obtain  $S(t)$  and  $n_c(t)$  through numerical simulation, which are shown in Figs. 7 and 8, respectively. We see that these results are generally consistent with those in Figs. 1 and 2. Note that the shape of the curves is slightly different between Figs. 2(c) and 8(c). The reason is that in the calculation we assume the number of packets in the queue follows a Poisson distribution, while it might not be always like this in real situations.

- [1] A. Klopper, *Nat. Phys.* **12**, 287 (2016).
- [2] A. Solé-Ribalta, S. Gómez, and A. Arenas, *Phys. Rev. Lett.* **116**, 108701 (2016).
- [3] Z. Toroczkai and K. E. Bassler, *Nature (London)* **428**, 716 (2004).
- [4] J. Zhao, D. Li, H. Sanhedrai *et al.*, *Nat. Commun.* **7**, 10094 (2016).
- [5] S. V. Buldyrev, R. Parshani, G. Paul *et al.*, *Nature (London)* **464**, 1025 (2010).
- [6] W. X. Wang and G. Chen, *Phys. Rev. E* **77**, 026101 (2008).
- [7] P. Crucitti, V. Latora, and M. Marchiori, *Phys. Rev. E* **69**, 045104 (2004).
- [8] Y. Berezin, A. Bashan, M. M. Danziger *et al.*, *Sci. Rep.* **5**, 8934 (2015).
- [9] C. Pu, S. Li, A. Michaelson *et al.*, *Phys. Lett. A* **379**, 1633 (2015).
- [10] C. L. Pu and W. Cui, *Physica A* **419**, 622 (2015).
- [11] R. Albert, H. Jeong, and A. L. Barabási, *Nature (London)* **406**, 378 (2000).
- [12] C. Pu, S. Li, X. X. Yang *et al.*, *Physica A* **446**, 129 (2016).
- [13] Z. Shen, S. Cao, W.-X. Wang, Z. Di, and H. E. Stanley, *Phys. Rev. E* **93**, 032301 (2016).
- [14] R. Pastor-Satorras, C. Castellano, P. Van Mieghem *et al.*, *Rev. Mod. Phys.* **87**, 925 (2015).
- [15] R. Pastor-Satorras, *Nat. Phys.* **11**, 528 (2015).
- [16] H.-X. Yang, M. Tang, and Y.-C. Lai, *Phys. Rev. E* **91**, 062817 (2015).
- [17] R. Pastor-Satorras and A. Vespignani, *Phys. Rev. Lett.* **86**, 3200 (2001).
- [18] S. Chen, W. Huang, C. Cattani, and G. Altieri, *Math. Probl. Eng.* **2012**, 732698 (2012).
- [19] B. Tadić, G. J. Rodgers, and S. Thurner, *Int. J. Bifurcat. Chaos* **17**, 2363 (2007).
- [20] L. Zhao, Y.-C. Lai, K. Park, and N. Ye, *Phys. Rev. E* **71**, 026125 (2005).
- [21] A. Arenas, A. Díaz-Guilera, and R. Guimera, *Phys. Rev. Lett.* **86**, 3196 (2001).
- [22] G. Yan, T. Zhou, B. Hu, Z.-Q. Fu, and B.-H. Wang, *Phys. Rev. E* **73**, 046108 (2006).
- [23] R. Guimerà, A. Díaz-Guilera, F. Vega-Redondo, A. Cabrales, and A. Arenas, *Phys. Rev. Lett.* **89**, 248701 (2002).
- [24] A. L. Barabási, *Science* **325**, 412 (2009).
- [25] Z. Liu, M.-B. Hu, R. Jiang, W.-X. Wang, and Q.-S. Wu, *Phys. Rev. E* **76**, 037101 (2007).
- [26] G. Q. Zhang, D. Wang, and G. J. Li, *Phys. Rev. E* **76**, 017101 (2007).
- [27] W. Huang and T. W. S. Chow, *J. Stat. Mech.* (2010) P01016.
- [28] W. Huang and T. W. S. Chow, *Chaos* **20**, 033123 (2010).
- [29] B. Awerbuch, in *Proceeding of the SIGCOMM'90 ACM Symposium on Communications Architectures & Protocols* (ACM, New York, 1990), Vol. 20, pp. 177–187.
- [30] Z. X. Wu, G. Peng, W. M. Wong *et al.*, *J. Stat. Mech.* (2008) P11002.
- [31] W.-X. Wang, B.-H. Wang, C.-Y. Yin, Y.-B. Xie, and T. Zhou, *Phys. Rev. E* **73**, 026111 (2006).
- [32] P. Echenique, J. Gomez-Gardenes, and Y. Moreno, *Phys. Rev. E* **70**, 056105 (2004).
- [33] H. Zhang, Z. H. Liu, M. Tang *et al.*, *Phys. Lett. A* **364**, 177 (2007).
- [34] X. Ling, M.-B. Hu, R. Jiang, and Q.-S. Wu, *Phys. Rev. E* **81**, 016113 (2010).
- [35] D. Wang, Y. Jing, and S. Zhang, *Physica A* **387**, 3001 (2008).
- [36] W.-X. Wang, C.-Y. Yin, G. Yan, and B.-H. Wang, *Phys. Rev. E* **74**, 016101 (2006).
- [37] W. Huang and T. W. S. Chow, *Chaos* **19**, 043124 (2009).
- [38] B. Tadić and S. Thurner, *Physica A* **332**, 566 (2004).
- [39] S. J. Yang, *Phys. Rev. E* **71**, 016107 (2005).
- [40] C. Pu, S. Li, X. Yang *et al.*, *Physica A* **447**, 261 (2016).
- [41] Y. Zhuo, Y. Peng, C. Liu *et al.*, *Physica A* **390**, 2401 (2011).
- [42] F. Tan, J. Wu, Y. Xia, and C. K. Tse, *Phys. Rev. E* **89**, 062813 (2014).
- [43] X. Nian and H. Fu, *Physica A* **410**, 421 (2014).
- [44] W. B. Du, X. L. Zhou, M. Jusup *et al.*, *Sci. Rep.* **6**, 19059 (2016).
- [45] W. B. Du, X. L. Zhou, Z. Chen *et al.*, *Chaos Soliton. Fract.* **68**, 72 (2014).
- [46] J. Zhou, G. Yan, and C. H. Lai, *Europhys. Lett.* **102**, 28002 (2013).
- [47] M. Cardei and D. Z. Du, *Wireless Netw.* **11**, 333 (2005).
- [48] I. Dietrich and F. Dressler, *ACM Trans. Sensor Netw.* **5**, 5 (2009).
- [49] I. F. Akyildiz, W. Su, Y. Sankarasubramaniam, and E. Cayirci, *IEEE Commun. Mag.* **40**, 102 (2002).
- [50] G. Calinescu, S. Kapoor, A. Olshevsky, and A. Zelikovsky, in *Proceedings of the 11th Annual European Symposium, Budapest, Hungary*, edited by G. Di Battista and U. Zwick, Lecture Notes in Computer Science Vol. 2832 (Springer, Berlin, Heidelberg, 2003), pp. 114–126.
- [51] M. Maleki, K. Dantu, and M. Pedram, in *Proceedings of the 2002 International Symposium on Low Power Electronics and Design* (ACM, New York, 2002), pp. 72–75.
- [52] M. Abolhasan, T. Wysocki, and E. Dutkiewicz, *Ad Hoc Netw.* **2**, 1 (2004).
- [53] I. Chlamtac, M. Conti, and J. J. N. Liu, *Ad Hoc Netw.* **1**, 13 (2003).
- [54] H. X. Yang and M. Tang, *Physica A* **402**, 1 (2014).
- [55] Y. Chen and Q. Zhao, *IEEE Commun. Lett.* **9**, 976 (2005).
- [56] M. Andjelković, N. Gupte, and B. Tadić, *Phys. Rev. E* **91**, 052817 (2015).